A simple approach to fabricate protective coatings on the surface of AZ91 alloy and its corrosion resistance

Bo Wang[1], Fengguang Zuo[2], Dixing Bai[3], Yingchen Yang[4], Cheng Li[5], Jumei Zhang[6]
[1, 2, 3, 4]State Grid Shaanxi Electric Power Research Institute, Xi'an, 710100, Shaanxi, China
[5]State Grid Shaanxi Electric Power Company Hanzhong Power Supply Company, Hanzhong, 723000, Shaanxi, China
[6]School of Materials Science and Engineering, Xi'an University of Science and Technology, Xi'an, 710054, Shaanxi, China
[1]Corresponding author
E-mail: [1]*wangjz012@yeah.net*, [2]*181696114@qq.com*, [3]*2963941563@qq.com*, [4]*yangyingchen01@163.com*, [5]*179231821@qq.com*, [6]*feiyue-zjm@163.com*

Received 18 November 2022; received in revised form 1 December 2022; accepted 6 December 2022
DOI https://doi.org/10.21595/vp.2022.23083

Check for updates

62nd International Conference on Vibroengineering in Almaty, Kazakhstan, February 10-11, 2023

Abstract. In this paper, the corrosion resistant coatings were fabricated on AZ91 Mg alloy by steam treatment using deionized water as a steam source. The treatment temperature was maintained at 150 °C, while the treatment time was varied at 3, 6 and 9 h. The results showed that relatively dense steam coating can be formed on the surface of AZ91 alloy by steam treatment for 3-9 h, and the phase structure of steam coating was mainly composed of $Mg(OH)_2$ and contained AlO(OH) and Mg-Al LDH. With the extension of the steam treatment time, the better the corrosion resistance of the steam coating, and the corrosion current density was as low as 10^{-7}~10^{-8} A·cm^{-2}, which was 3-4 orders of magnitude lower than AZ91 Mg alloy substrate (~10^{-4} A·cm^{-2}).

Keywords: magnesium alloy, steam treatment, steam coating, corrosion resistance.

1. Introduction

Magnesium alloy is the lightest metal structure material, which is the ideal material to realize lightweight equipment [1-2]. However, the poor corrosion resistance of magnesium alloy is the main obstacle for its wide application in industrial products [3-4]. Therefore, improving the corrosion resistance of magnesium alloy is of great significance to expand the application of magnesium alloy. A large number of studies have proved that surface treatment techniques such as micro-arc oxidation (MAO), Ni-P electroless plating and hydrothermal treatment can improve the corrosion resistance of magnesium alloys [5-7]. However, a major drawback of the above surface treatment methods is the unavoidable use of multiple chemical reagents in the treatment process. Micro arc oxidation treatment also needs special equipment, and the energy consumption is high in the process of treatment. Therefore, the above surface treatment methods not only lead to high preparation cost of protective coating, but also bring environmental pollution risk due to the involvement of heavy metal ions.

Steam treatment is a truly low-cost and environmentally friendly treatment method because no chemicals are used and only water is used as the steam source. Therefore, in this paper, commercial AZ91 Mg alloy widely used in industry is taken as the research object, and treated by steam treatment at 150 °C for different time using pure water as the steam source. The main research objective of this work is to study the effect of steam treatment time on the structure, morphology and corrosion resistance of the obtained steam coating.

2. Materials and experimental procedure

AZ91 Mg alloy (composition: 9 wt.% Al, 1 wt.% Zn, 0.3 wt.% Mn, and balance Mg) with a

size of Φ20 mm×5 mm was used as experimental material. The polished and cleaned AZ91 alloy was placed on a Teflon tube in a Teflon-lined autoclave with a 25 mL capacity, and 5 mL of pure water was added to the bottom of the autoclave to produce steam. The autoclaves were put into a drying oven after tightening and were heated at 150 ℃ for 3, 6 and 9 h. It was then cooled naturally to room temperature. After the steam treatment, the films coated on AZ91 substrates were taken out, and the obtained samples were labeled as 150 ℃-3 h, 150 ℃-6 h and 150 ℃-9 h, respectively.

The phase structure of the steam coatings as well as AZ91 substrate were identified using X-ray diffraction (XRD, PANalytical, Aeris, Holland). The morphologies and chemical composition of steam coatings treated at different time were observed using a field emission scanning electronic microscope (SEM, Merlin Compact, Germany) and energy dispersive X-ray spectrometer (EDS, Oxford Instruments, Britain). The cross section morphology of the coating was observed by TESCAN VEGA3 XMU scanning electron microscope. Finally, the electrochemical characteristics of steam coatings treated at different time and untreated AZ91 alloy were estimated by measuring potentiodynamic polarization curves and electrochemical impedance spectra (EIS) in 3.5wt% NaCl solution at room temperature with a typical three-electrode system.

3. Results and discussions

XRD Results and Macromorphology of Steam Coatings Prepared on AZ91 Alloy. The XRD patterns and macromorphology of bare AZ91 alloy and steam coatings prepared by treated at 150℃ for different time are demonstrated in Fig. 1. Compared to the appearance of bare AZ91 alloy, the surface was uniformly covered with a matt film, which had been successfully prepared the steam coating on the surface of AZ91 alloy. For the bare AZ91 Mg alloy, some peaks attributable to α-Mg (ICDD-PDF No. 00-035-0821) were clearly observed at 2θ = 32.28°, 34.48°, 36.73°, 47.93°, 57.40°, 63.22°, 64.29°, 68.82° and 70.17°. In addition, small peaks attributable to β-Mg17Al12 (ICDD-PDF No. 01-073-1148) were also detected at 2θ = 35.84°, 39.74°, 41.61°and 43.36°. These results indicate that the bare AZ91 Mg alloy is composed of two different phase constituents, α-Mg and β-Mg17Al12. However, for the steam coatings prepared by treated at 150 ℃ for different time, some peaks observed at around 2θ = 18.41°, 32.72°, 37.86°, 50.66°, 58.42°, 61.82° and 71.74° in all XRD patterns are assigned to the 001, 100, 101, 102, 110, 111 and 201 reflect of brucite-type $Mg(OH)_2$ (ICDD-PDF No. 01-044-1482). The peaks at around 2θ = 14.39° and 27.99° observed in the XRD patterns were attributable to the 020 and 021 reflections of bohmite-type AlO(OH) (ICDD-PDF No. 01-074-1895). Except for the previously mentioned peaks, two peaks at approximately 2θ = 11.65° and 23.00° associated with the 003 and 006 reflections of the carbonate type Mg-Al LDH (ICDD-PDF No. 01-070-2151) were clearly observed. These results suggested that the steam coatings coated on AZ91 alloy were composed of a mixed structure of $Mg(OH)_2$, AlO(OH) and Mg-Al LDH phases. The relevant reaction equations are shown in the Eq. (1-4):

$$Mg - 2e^- \rightarrow Mg^{2+}, \quad (1)$$

$$Mg^{2+} + 2OH^- = Mg(OH)_2, \quad (2)$$

$$Al^{3+} + 4OH^- = Al(OH)_4^-, \quad (3)$$

$$2Mg^{2+} + Al(OH)_4^- + 3OH^- + 2H_2O \rightarrow Mg_2Al(OH)_7 \cdot 2H_2O. \quad (4)$$

Surface and Cross-Sectional SEM Morphology of Steam Coatings Prepared on AZ91 Alloy. Fig. 2 displays the surface SEM morphology and corresponding EDS spectrum of AZ91 alloy after steam treatment for different time. As can be seen from Fig. 2(a-c), the surface of the all coatings were uniform and dense without any pore or crack. There was obvious change in the morphology with changing treatment time. The size of the nanosheets obtained by the longer treatment was significantly larger than that of the shorter treatment. These results confirmed that the $Mg(OH)_2$, AlO(OH) and Mg-Al LDH were formed and covered throughout the substrate

surface by steam treatment. The EDS results revealed that the composition of steam coating was composed of C, O, Mg and Al elements. Among them, Mg and Al elements come from AZ91 alloy matrix, while C and O elements come from air and water vapor in the sealed autoclave.

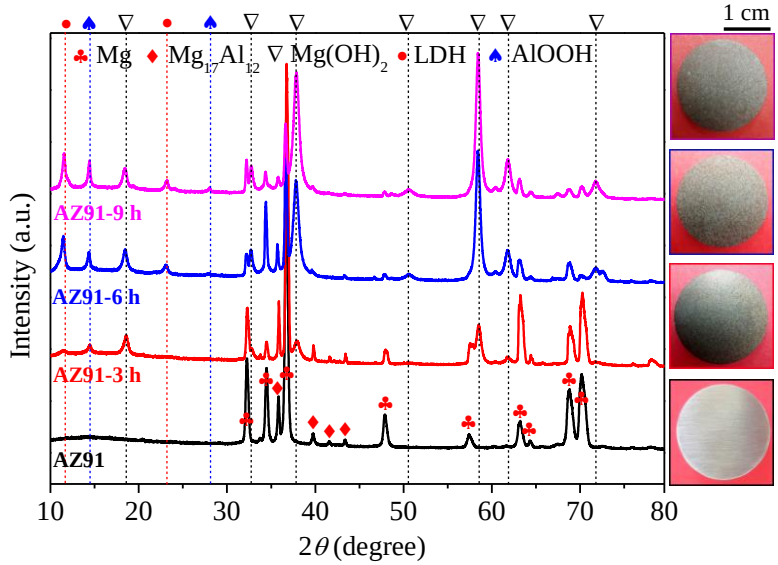

Fig. 1. XRD patterns and macromorphology of AZ91 alloy before and after steam treatment for different time

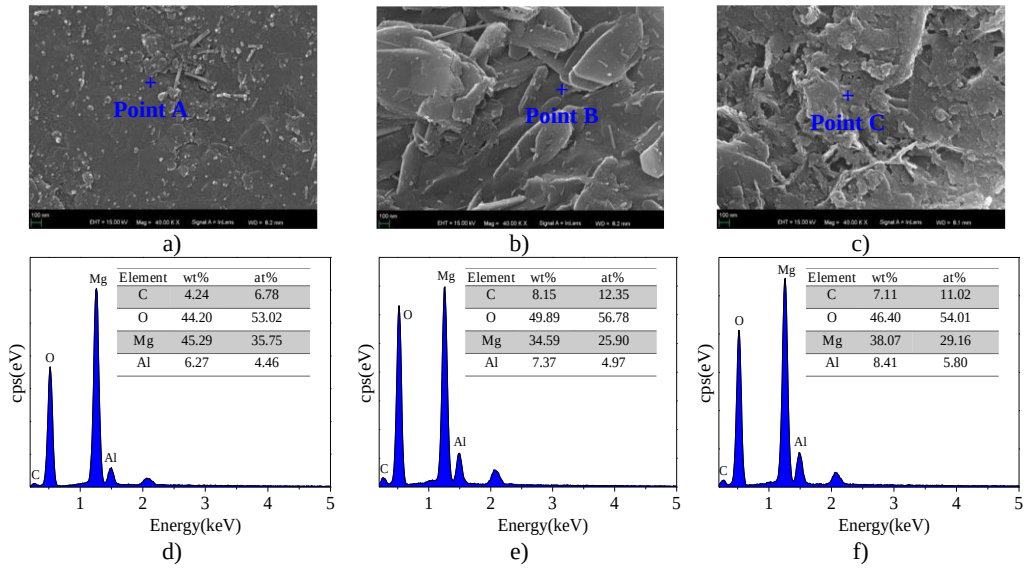

Fig. 2. Surface SEM morphologies and EDS spectrum of AZ91 alloy after steam treatment for different time a), d) AZ91-3 h; b), e) AZ91-6 h; c), f) AZ91-9 h

The cross-sectional SEM images of all films are shown in Fig. 3. It was seen that the coatings between 3 and 9 h were dense although some cracks or pores could be observed with an increase in treatment time. The β-$Mg_{17}Al_{12}$ phase between the coating and the substrate was also observed. As the processing time increased from 3 h to 9 h, the average thickness of the coating increased from 8 μm to 71 μm. It was noteworthy that the coating thickness increased rapidly when the treatment time exceeded 3 h. However, when the treat time was more than 6 h, the increase rate

of coating thickness tended to be gentle. This phenomenon may be related to the increased difficulty of steam permeating into the coating and eventually reaching the substrate surface.

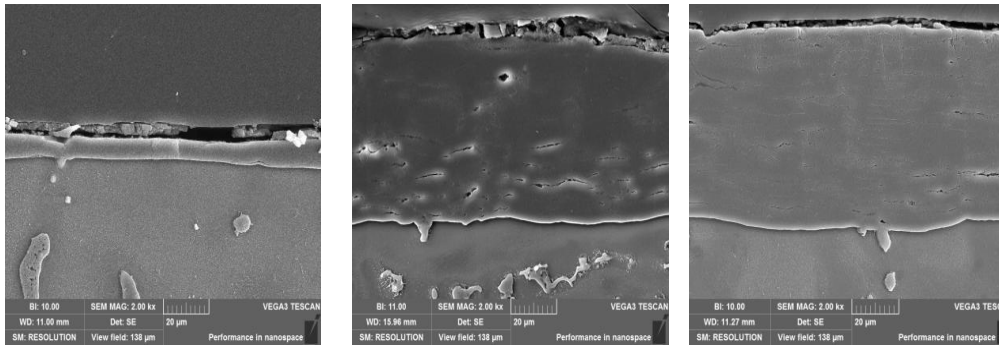

a) AZ91-3 h b) AZ91-6 h c) AZ91-9 h

Fig. 3. Cross-sectional SEM morphology of AZ91 alloy after steam treatment for different time

Corrosion Resistance of Steam Coatings Prepared on AZ91 Alloy. The Bode plots, nyquist plots and polarization curves of AZ91 alloy and steam coatings prepared by treated at 150 ℃ for different time in 3.5 wt% NaCl aqueous solutions are depicted in Fig. 4. It is well known that the Bode plot with a large impedance modulus at low frequency, such as $f = 0.01$ Hz (|Z| $f = 0.01$ Hz), indicates an excellent corrosion resistance [7]. It is evident from in Bode plot shown in Fig. 4(a) that the |Z| $f = 0.01$ Hz for bare AZ91 Mg alloy is only 3.37×102 Ω·cm^2, whereas the |Z| $f = 0.01$ Hz for all steam coatings are greater than that of bare AZ91 Mg alloy, which is increased by 3-4 orders of magnitude in comparison with bare AZ91 Mg alloy. 150 ℃+9 h coating shows the highest |Z| $f = 0.01$ Hz value (2.29×106 Ω·cm^2), followed by 150 ℃+6 h coating (1.96×106 Ω·cm^2) and 150 ℃+3 h coating (8.70×105 Ω·cm^2). That is to say, the longer the treatment time is, the higher the |Z| $f = 0.01$ Hz is, and the better the corrosion resistance is. Of course, there is little difference between the two |Z| $f = 0.01$ Hz values of 150 ℃+9 h coating and 150 ℃+6 h coating.

The Nyquist plots of bare AZ91 alloy and three steam coatings are displayed in Fig. 4(b) and Fig. 4(c), respectively. It is generally assumed that the larger the impedance loop in the Nyquist plots at low frequency, the better anticorrosive the material would be [7, 8]. It can be observed from Fig. 4(b) and Fig. 4(c) that the steam coatings have larger impedance at low frequency compared with the bare AZ91 Mg alloy, which indicates the best corrosion resistance. What's more, along with the increase of the steam treatment time, the impedance at low frequency increase. The corresponding equivalent circuits (ECs) of bare AZ91 Mg alloy and steam coatings are given in Fig. 4(b) and Fig. 4(c), and the fitting results are plotted by solid curves in Fig. 4(a-c).

Fig. 4(d) depicts the polarization curves and electrochemical fitting parameters (corrosion potential Ecorr and corrosion current density Icorr) of bare AZ91 and three steam coatings, which are employed to investigate the corrosion resistance of the steam coatings as well as the bare AZ91 in 3.5 % NaCl aqueous solution. In contrast to bare AZ91 alloy, the values of βa (anodic Tafel slope) of steam coatings were significantly increased and the breakdown potential seemed to be appeared, suggesting that the steam coatings prevented the anodic reaction [7]. According to the results, the I_{corr} values of bare AZ91 and three steam coatings can be ranged in decreasing order: bare AZ91 > 150 ℃+3 h > 150 ℃+6 h >150 ℃+9 h. The Icorr values of steam coatings decreased by 3-4 orders of magnitude relative to the bare AZ91, and the Ecorr values slightly moved in the positive direction. The lower the Icorr value and the greater the Ecorr value is, the better the corrosion resistance of the coating gets [9]. The results showed that the corrosion resistance of AZ91 alloy can be improved significantly by the steam coatings. It's worth noting that the corrosion resistance of 150 ℃+9 h coating was slightly better than that of 150 ℃+6 h coating. The results are consistent with the previous EIS analysis.

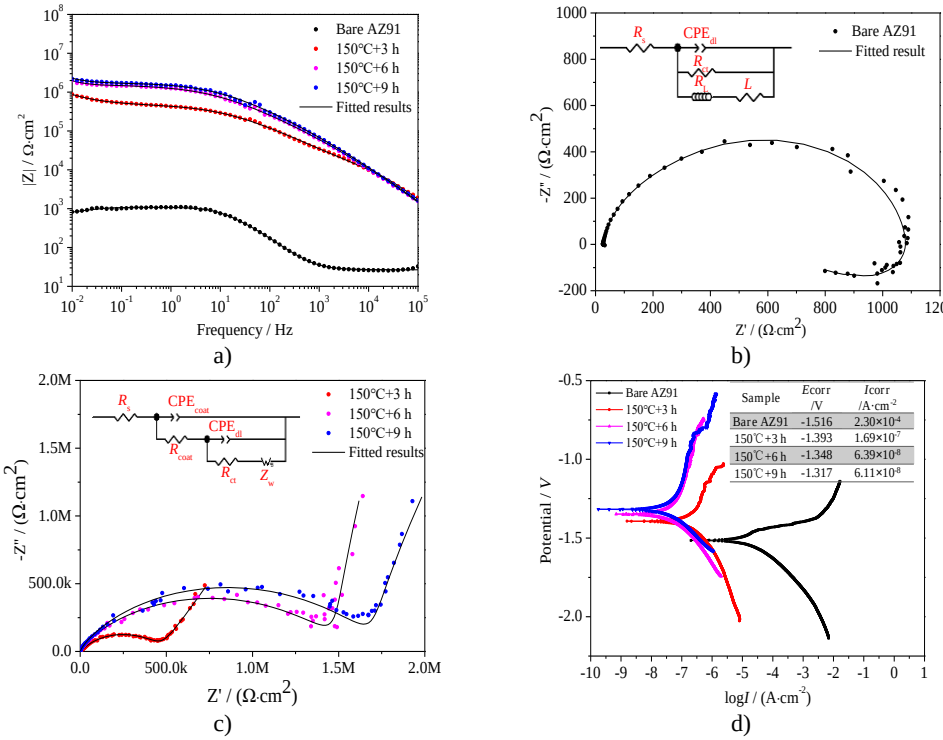

Fig. 4. Bode plots, nyquist plots and polarization curves of AZ91 alloy and steam coatings: a) Bode plots; b) Nyquist plots of AZ91 alloy; c) Nyquist plots of steam coatings; d) Polarization curves

4. Conclusions

We have prepared the high corrosion resistant coatings on AZ91 Mg alloy using a simple steam treatment. The steam coatings exhibited a mixed structure of $Mg(OH)_2$, AlO(OH) and Mg-Al LDH phases as determined by XRD analysis. The SEM result displayed that the steam coating surface was relatively dense. With the extension of the steam treatment time, the average thickness of the steam coating increased significantly. The corrosion resistance of the coatings evaluated by EIS and polarization curves in 3.5 wt% NaCl aqueous solutions demonstrated that the coating prepared at 6 h or 9 h revealed the most superior protective behavior. The high corrosion resistant performance was mainly attributed to denseness and thickness of the steam coating.

Acknowledgements

The authors have not disclosed any funding.

Data availability

The datasets generated during and/or analyzed during the current study are available from the corresponding author on reasonable request.

Conflict of interest

The authors declare that they have no conflict of interest.

References

[1] T. Xu, Y. Yang, X. Peng, J. Song, and F. Pan, "Overview of advancement and development trend on magnesium alloy," *Journal of Magnesium and Alloys*, Vol. 7, No. 3, pp. 536–544, Sep. 2019, https://doi.org/10.1016/j.jma.2019.08.001

[2] W. J. Joost and P. E. Krajewski, "Towards magnesium alloys for high-volume automotive applications," *Scripta Materialia*, Vol. 128, pp. 107–112, Feb. 2017, https://doi.org/10.1016/j.scriptamat.2016.07.035

[3] K. Cao et al., "Fabrication of superhydrophobic layered double hydroxide composites to enhance the corrosion-resistant performances of epoxy coatings on Mg alloy," *Surface and Coatings Technology*, Vol. 407, p. 126763, Feb. 2021, https://doi.org/10.1016/j.surfcoat.2020.126763

[4] Y. He, C. Peng, Y. Feng, R. Wang, and J. Zhong, "Effects of alloying elements on the microstructure and corrosion behavior of Mg-Li-Al-Y alloys," *Journal of Alloys and Compounds*, Vol. 834, p. 154344, Sep. 2020, https://doi.org/10.1016/j.jallcom.2020.154344

[5] Z. Dou et al., "Insight into chelating agent stimulated in-situ growth of MgAl-LDH films on magnesium alloy AZ31: The effect of initial cationic concentrations," *Surface and Coatings Technology*, Vol. 439, p. 128414, Jun. 2022, https://doi.org/10.1016/j.surfcoat.2022.128414

[6] Z.-H. Wang, J.-M. Zhang, Y. Li, L.-J. Bai, and G.-J. Zhang, "Enhanced corrosion resistance of micro-arc oxidation coated magnesium alloy by superhydrophobic Mg-Al layered double hydroxide coating," *Transactions of Nonferrous Metals Society of China*, Vol. 29, No. 10, pp. 2066–2077, Oct. 2019, https://doi.org/10.1016/s1003-6326(19)65113-7

[7] G. Zhang et al., "Active corrosion protection by a smart coating based on a MgAl-layered double hydroxide on a cerium-modified plasma electrolytic oxidation coating on Mg alloy AZ31," *Corrosion Science*, Vol. 139, pp. 370–382, Jul. 2018, https://doi.org/10.1016/j.corsci.2018.05.010

[8] J. Zhang et al., "A comparative study and optimization of corrosion resistance of Mg-Al layered double hydroxides films at different hydrothermal temperatures on LA103Z Mg-Li alloy," *Materials and Corrosion*, pp. 1–11, Oct. 2022, https://doi.org/10.1002/maco.202213543

[9] J. Zhang et al., "In situ growth process and corrosion resistance of a layered double-hydroxide film on an LA103Z magnesium-lithium alloy," *Materials and Corrosion*, Vol. 73, No. 7, pp. 1099–1109, Jul. 2022, https://doi.org/10.1002/maco.202113022